SPATIOTEMPORAL MODELLING & AUTOMATED *IN-SITU* SENSORS TO MONITOR HARMFUL ALGAL BLOOMS (HABS)

Case Study Lake Victoria

by

Okomo Jacob Okello

Project report submitted to the department of Geomatic Engineering and Geospatial Information Systems degree of Bachelor of Science in Geospatial Information Sciences (GIS), 2021

Department of Geomatic Engineering and Geospatial Information Systems (GEGIS)

DECLARATION

I declare that this project is my own work and has not been submitted by anybody else in any other university for the award of any degree to the best of my knowledge.

Sign…………………………… Date…………………………………...

Jacob Okello Okomo

ENC222-0149/2017

Department of Geomatic Engineering and Geospatial Information Systems (GEGIS)

Jomo Kenyatta University of Agriculture and Technology

CERTIFICATION

This project has been submitted for examination with my approval as the candidate's supervisor.

Sign…………………………. Date …………………………………………

Dr. Eunice Nduati

Senior Lecturer, GEGIS

Department of Geomatic Engineering and Geospatial Information Systems (GEGIS)

Acknowledgements

The achievement(s) in this thesis submission were not fully accomplished solely by the student author. A number of individuals helped me with mentorship and logistical support during the process.

First and foremost, I'd want to express my sincere gratitude to my major advisor and supervisor, Dr. E. Nduati form Department of Geomatic Engineering and Geospatial Information Systems-GEGIS. Your enormous energy and enthusiasm serve as a constant reminder of what I enjoy about geoscience. Thank you very much. You deserve special recognition. Both professionally and emotionally, you have been an amazing role model for me. You believed in my ideas and gave me the freedom to pursue them. Working under your guidance has provided me with the resources and confidence I need to accomplish my career achievements.

I sincerely thank Google Earth Engine and United States Geological Survey (USGS) for the provision of Satellite Remote sensing images, particularly Landsat 8 image collection that came in handy for this project realization.

Sincere gratitude is as well sent to Kenya Marine and Fisheries Research Institute (KMFRI) for providing a tone of information that are directly in line with this project.

I would as well like to acknowledge the efforts of both teaching and non-teaching staff from the Department of GEGIS who directly impacted me with knowledge in various aspects and skills that have played key roles in my project. To you all, may you be blessed abundantly.

Abstract

This is meant to cover the whole project content in brief. I therefore request to update this section at project completion and closure stage.

-Thank you

Table of contents

List of figures

List of tables

Acronyms and abbreviations

1. DO — Dissolved Oxygen
2. DN — Digital Numbers
3. GDP — Gross Domestic Product
4. GEGIS — Geomatic Engineering and Geospatial Information Systems
5. HAB — Harmful Algal Bloom
6. FAI — Floating Algae Index
7. FLH — Fluorescence Line Height
8. IoT — Internet of Things
9. KMFRI — Kenya Marine and Fisheries Research Institute
10. KTN — Kenya Television News
11. LSAT — Lake Surface Air Temperature
12. LSWT — Lake Surface Water Temperature
13. MCI — Maximum Chlorophyll Index
14. MERIS — MEdium Resolution Imaging Spectroradiometer
15. ML — Machine Learning
16. MODIS — MODerate Resolution Imaging Spectrometer
17. OLI — Operational Land Imager
18. OC — Ocean Color
19. Quick-SCAT — Quick Scatterometer
20. SeaWiFS — Sea-viewing Wide-Field- of-View Sensor
21. SST — Sea Surface Temperature
22. TIRS — Thermal InfraRed Sensor
23. USGS — United States Geological Survey

1 Introduction

1.1 Background

Richardson K. (1997) defined Algal bloom as "the rapid growth of one or more species which leads to an increase in biomass of the species". This is normally associated with high concentrations of phytoplankton (algae). If the rapid growth is related to a toxic or harmful species, then the phenomenon can be termed as Harmful Algal Bloom (HAB). A species can be harmful due to the release of toxic substances e.g., *Cyanotoxins spp*. which are the most frequent in the Lake Victoria region (Okello et al., 2011). Often termed as "Red Tides", HABs have attracted a significant world-wide attention in research over the last two decades (W. Song et al.,2015; Manuel et al., 2020).

Development, stability, and density of the phenomenon are related to some environmental factors such as wind velocity and direction, Lake Surface Water Temperature (LSWT), Lake Surface Air Temperature (LSAT), Sea Surface Temperature (SST), currents, and adequate nutrient concentration, enough sunlight, warm temperatures (Tang et al, 2006) to be transported over a water body e.g., Kisumu Bay by local circulations and winds especially in large aggregates called *colonies* (Okello & Kurmayer, 2011).

A lot of scholars in the geosciences have put forward a bunch of approaches to detect and monitor HABs in both inland and ocean waters including generating indices from spectral band ratio algorithms e.g., Empirical visible-NIR band ratios (Matthews et al, 2012; Allan et al, 2015), blue-green band ratios (O'Reilly et al., 1998), red-edge (RE) region (685–720 nm) band ratios (Mittenzwey et al., 1992), thermal band based assessment (Tang et al.,2006) can be exploited to detect and monitor occurrence of a variety of HABs.

Currently, remote sensing of HAB detection and monitoring methods are primarily designed for sensors like MODIS, MERIS and SeaWiFS, (Kurekin et al., 2014) which despite allowing us to continuously monitor the behavior of the phenomenon (due to high temporal resolution (about 1 day revisit time), limits us from a detailed

examination of HABs (due to coarse spatial resolutions (250~1130 meters) and only large scale HABs can be monitored by using them (Blondeau, 2014).

Landsat 8 OLI being able to discriminate finer details, therefore possesses the great value and potential to provide for the retrieval of Chl-a at 3om spatial resolution (Allan et al., 2015; Watanabe et al., 2015; Concha and Schott 2016; Manuel et al., 2020).

The advent and uptake of Internet of Things (IoT) further provides for quick development of geo-intelligent automated in-situ sensors that collects near real-time water quality data e.g., LSWT, LSAT which are thermal proxies and indicators of HAB presence thereby enabling a step-change in data availability for HAB monitoring in Lake Victoria.

Therefore, an approach that utilizes high spatiotemporal sensor's capability to detect and monitor HABs coupled by in-situ sensors technically sounds essential. Landsat 8 high spatiotemporal satellite images (30 & 100 meters for spatial resolution and 16 days for temporal) have advanced the space-based capabilities in detection and monitoring of HABs comparatively more accurately at relatively smaller inland water bodies e.g., Nyanza Gulf of Lake Victoria.

On that regard, this study intends to demonstrate the potential of using spectral bands 2, 3, 4, 5 and TIR band 10 of L8 OLI in detecting and monitoring of HABs using empirical statistical methods.

1.2 Motivation and problem statement

Harmful Algal Blooms continue to be a major source of concern, not only because of their huge environmental and socioeconomic consequences, but also because of a recent dramatic increase in the number of cases documented around the world (Hill et al., 2020). HABs have the potential to cause serious environmental and human health issues, as well as other complications in deterioration of economic status thereby impacting a region's GDP. Environmental impacts include depletion of dissolved oxygen (DO) in the aquatic habitat causing mass fish stock (Tang et al, 2006) (*Fig 1,2,3 below*). Impacts posed to human inhabitants include toxic reactions to affected seafood and even in extreme cases, fatalities. Related economic impacts include adverse effects on coastal based industries e.g., fishing (Smith et al., 2019), tourism (*Fig 4*).

Lately, coastal regions of Lake Victoria especially around Nyanza Gulf (Kisumu Bay) have shown deterioration in its water quality as seen in severe signs of eutrophication with blooms (Simiyu et al., 2018).HABs can be caused by a variety of circumstances, but they are most commonly associated with favorable environmental conditions, such as increased nutrient levels-eutrophication (Santoleri et al., 2003), which are generally driven by urbanization, deforestation and poor agricultural practices (Gohin F. et al., 2006; Hecky et al., 2010).

1.3 Justification

One of the bays of Lake Victoria that is mostly affected by nutrient enrichment is Nyanza Gulf (Gikuma-Njuru, P. 2013) which is discharged from the densely populated catchment with mostly subsistence agriculture (Calamari, D. 1995; Hecky, R.E. 2010). This has led to regular occurrence of bloom-forming cyanobacteria which has been associated with mass fish kills *(Fig 1, 2 & 3 below)* due to depletion of dissolved oxygen (DO) in the aquatic habitats and to some extremes, temporary shutdown of drinking water supply, i.e., from January to March 2004 (Sitoki et al., 2012).

For this purpose, a number of Landsat 8 images with some acquired in a bloom event and some during a non-bloom condition will be quantitatively analyzed. By comparing the statistically derived numerical values of the spectral indices in blooming and non-blooming condition, indices and thermal information will be extracted.

Fig 1: Standard Media Kenya reports through KTN about HABs causing Mass Fish stocks in Dunga Beach Kisumu region in February 2021, (Image: Standard Media KE)

Fig 2: Mass fish stock in Lake Victoria Shores impacted by the HABs (Image: Standard Media KE)

Fig 3: High valued Fish lost to HAB in Lake Victoria Shores (Image Source: KMFRI)

Fig 4: Tourism and therefore Income halted to HABs

1.4 Research identification and Objectives

The main objective of this research is to detect, monitor and report the occurrence of Harmful Algal Blooms (HABs) and Cyanobacteria in Lake Victoria. This is achievable through the following specific objectives:

1.4.1 Research objectives

1   To monitor the distribution of chlorophyl-a(Chl-a) concentrations from L8 OLI data as HAB proxies in L. Victoria from 2015 to 2021.

2   To monitor Lake Surface Air Temperature (LSAT) and Lake Surface Water Temperature (LSWT) from L8 TIRS images as another HAB indicator in L. Victoria.

3   To develop automated Internet of Things (IoT) *in situ* sensors, applicable in near real-time to monitor and report geo-tagged Water quality data (e.g., LSWT) from 2021 onwards.

1.4.2   Research questions

The following questions are formulated with respect to aforementioned objectives:

1) Can space based observation systems be used to detect and monitor HABs in Lake Victoria Inland water body?
2) Does HAB occurrence have a direct impact on the LSAT and LSWT at their point of influence?
3) Can IoT be utilized to monitor HAB occurrences inland water Lakes?

1.5 Study outline

This research study is intended to be divided into 6 chapters whereby the first chapter introduces the study by detailing into the background, motivation and problem statement, justifying the problem, objectives and research questions; Chapter 2 contains the reviewed literature which relate to this thesis. Further, Chapter 3 will show the data and methods used in the study with Chapter 4 highlighting the results for the findings from the methods. Chapter 5 will discuss on the findings and finally, Chapter 6 will conclude and recommend for future research that might not be addressed at this level of geoscientific expertise.

2. Literature review

2.1 A Synthesis on the Occurrence and Negative Impacts of HABs

During the last few decades (especially the last two decades), eutrophication of lakes as a result of HABs has been a common environmental problem observed in both freshwater (Jiang et al. 2015; Luo et al. 2016) and salty water bodies (Blondeau-Patissier et al., 2014), raising a global concern due to their ability to rapidly produce various hepatotoxic and neurotoxic substances (W. Song et al.,2015).This has so been the case even at a local water bodies like Lake Victoria in East Africa which showed a potential significance of algal blooms reported as early as 1980's (Ochumba, 1984).

Proliferation of algae causes eutrophication of freshwater lakes under certain environmental conditions and float on the water surface to cause abnormal watercolor amongst a variety of aquatic-related threats (Huisman et al. 2005; Liu and Yang 2012; Qin et al. 2016). These phenomena have been observed to be severely detrimental to aquatic environment in global inland water bodies which generally follows to the growing discharge of domestic or industrial wastewater as well as agriculture and fertilizer runoff (Glibert et al., 2005; Tang et al, 2006).

The ecological phenomenon has apparently been related to a variety of socioeconomic havocs like widespread occurrence of mass fish stocks and fish booms (Ochumba, 1985, 1987; Caballero et al., 2020). Being actively photosynthetic, the blooms, not only deplete the dissolved oxygen (DO) in waters that result in mass death to water lives but also release toxins, e.g., microcystin, that cause health risks to wildlife, livestock, pets, and humans who get in contact with the HABs (Hallegraeff, 1993), affecting the safety of drinking water supply (Guo 2007; Qin et al. 2010) leading to the disruption of the water food chain as it affects both trophic levels in the chain (Diaz and Rosenberg 2008).

Furthermore, surface foams or scums formed by CyanoHABs and their odorous compounds foul up water quality and surrounding recreational environment (Anderson et al., 2002).

2.2 Space-based Optical Remote Sensing in the Monitoring of Chlorophyll-a as an indicator of HAB event.

Numerous geoscience scholars have observed that space-based observations are of great significance and importance in quantifying in detailed the spatiotemporal distributions of HABs in inland water bodies.

Surface-level concentrations of Chl-a, a proxy for HAB, has been quantitatively observed in aquatic ecosystems via the exploitation of optical remote sensing for many years (Clarke et al., 1970; Wezernak et al., 1976; Smith and Baker 1982; Gordon et al., 1983; O'Reilly et al., 1998; Tang et al., 2006; Gitelson et al., 2007; Allan et al., 2015; Watanabe et al., 2015; Concha and Schott 2016). This technique has routinely supported the generation of global Chl-a distributions maps for the oceans for more than two decades (W. Song et al.,2015; Manuel et al., 2020).

A wide variety of heritage algorithms have been developed in that regard. For example, the blue-green band-ratio models have been used to quantitatively asses Chl-a (Gordon et al., 1980; Bukata et al., 1995;).However, in optically more complex inland and coastal waters, the color of water is further modified by the dominance of organic and inorganic particles, as well as colored dissolved organic matter (CDOM) (Mittenzwey et al., 1992; Han et al., 1994; Harding et al., 1994) that do not generally co-vary with Chl-a.

Consequently, to improve the estimation of Chl-a in these eutrophic and turbid environments, more sensitive methodologies have been proposed and implemented. For instance, sensors that image within the Red Edge region (690–715 nm) of the EM spectrum (Vos et al., 1986; Mittenzwey et al., 1992), when combined with red bands have manifested at a greater confidence to correlate well with Chl-a in eutrophic and/or turbid waters (Munday and Zubkoff 1981; Gower et al., 1984; Khorram et al., 1987; Gitelson 1992; Rundquist et al., 1996; Gitelson et al., 2007).

The Operational Land Imager sensor aboard Landsat-8 which was commissioned into orbit in 2013, February to capture changes at relatively high (30 m) spatial resolution which is relatively high (Irons et al., 2012) has offered significant space observatory improvements in both data quality and quantity (i.e., both spectral and spatial

coverage) over other previous heritage optical sensors (Markham et al., 2014; Pahlevan et al., 2014; Markham et al., 2015) and is relatively capable of monitoring bimonthly HAB dynamics (Pahlevan et al., 2014; Allan et al., 2015).

Several methods have been developed to retrieve Chl-a from the four OLI visible bands (Markham et al., 2015; Watanabe et al., 2015; Concha and Schott 2016; Manuel et al., 2020).

2.2.1 Retrieval of Chl-a from Landsat 8 OLI Optical Spectral Bands

O'Reilly et al. (1998) observed that for satellite missions that do not inherently support measurements in the Red Edge portion of the EMR Spectrum, Chl-a algorithms tend to alternatively rely on blue-green band ratio algorithms coupled by some complex ML approaches. This is true even for Landsat-8 (Le et al., 2013; Markham et al., 2015; Freitas and Dierssen 2019).

Most research on Chl-a retrieval has heavily relied on missions like the MERIS, inherently designed to image in the RE portions (Gitelson 1992; Gower et al., 2005; Gitelson et al., 2007); These algorithms have however been noted not to score well to missions that are limited to such measurements (RE) like MODIS (Esaias et al., 1998), VIIRS (Wang et al., 2014), Geostationary Ocean Color Image (GOCI) (Ryu et al., 2012) and Landsat 8 (Snyder et al., 2017). Thus, the adoption of Empirical standard algorithms of the Ocean Color (OC) spectral band family for Chl-a estimation (e.g., OC3), (Neil et al., 2019) which has been proven to improve Chl-a retrieval from OLI products in highly eutrophic and even clear aquatic regions (Cao et al., 2020) like Kisumu Bay.

The Ocean Color 3 regional algorithms specific to OLI spectral imageries have been successfully implemented in lakes and reservoirs (Allan et al., 2015; Watanabe et al., 2015; Snyder et al., 2017) for chl-a retrieval.

2.3 Capabilities of Space-based observations in the Monitoring of Lake Surface Air Temperature (LSAT) as an indicator of HAB event.

With the advent of thermal imaging remote sensing, it has been observed that Sea Surface Temperature (SST) observations derived from space borne sensors like the Advanced very high-resolution radiometer (AVHRR) in conjunction with optically derived Chl-a data have great potential to detect and monitor HAB at an improved accuracy (Tang et al., 2003a; Thomas et al., 2012).

Thermal infrared bands are potentially capable of quantifying the amount of infrared radiant heat emitted from aquatic surfaces that have environmental and economic import (Anderson, J. et al., 1984; Haakstad, M. et al., 1994; River S et al., 2004).

It has been noted that Satellite Sea Surface Temperature (SST) data are often used in combination with chlorophyll-a to relate to bloom events (Villareal et al., 2012) at a higher accuracy. This has also been observed in inland water bodies where Lake Surface Air and Water Temperatures (LSAT and LSWT) are taken in considerations (Thomas et al., 2012; Shi and Wang, 2007). Peñaflor et al. 2007 also examined the correlation of seasonal phytoplankton bloom in the Luzon Strait off the Philippines using MODIS Chl and SST, in addition to Quick-SCAT wind data. Similar findings were also documented by Binding et al., 2012, 2013 by using MERIS MCI in particular by focusing in the FLH and FAI, as well as other indices, used in conjunction with satellite estimates of Chl-a and SST to improve our image analysis in a very efficient way.

Blooms of blue-green algae are reportedly often associated with increase in water temperatures (Hutchinson, 1967). During a bloom observed in Lake Victoria, the average Lake Surface Water temperature of the open waters rose from (23.9-24.8°C) to (26.9–29.5°C) in May of 1986 within two weeks of the bloom period (Kilham, 1991; Gasse, Talling & Kilham, 1994).

2.4 A Review of the Potential of Smart IoT Solutions in Location-based Water quality monitoring.

The advent of smart solutions and of Internet of Things (IoT) has lately shown an escalating curve in their great capability to monitor water quality particularly with advancement in communication technology (Jan et al., 2021). This has greatly improved the capabilities to remotely gather and disseminate the in-situ water parameters e.g., Lake Surface Water Temperature (LSWT) and Lake Surface Air Temperature (LSAT) (Cloete et al., 2016), which are correlated with an algal bloom event in inland water bodies.

In this regard, legislations have been passed through the relevant government and non-governmental agencies for example the Kenya Marine and Fisheries Research Institute (KMFRI), African Great Lakes to set thresholding standards in water quality parameters that relate to HAB events. These parameters include Lake Victoria Surface Air Temperature which is set to vary with the proximity from the shore, (25.5 +/- 5°**C**), Suspended solids (30 mg/L), Pathogens and bacteria (Nil/100ml), Fluoride (1.5mg/L), Total dissolved solids (1200mg/L), Ammonia (0.5 mg/L), Nitrates (10mg/L) (Budyko, M. I. 1974; Yin & Nicholson, n.d.), among many other water quality parameters.

In-situ Water quality monitoring is defined as the collection of information at set locations and at regular intervals in order to provide data which may be used to assess current conditions and even establish trends etc. (Yang et al., 2011; Encinas et al., 2017). This can be used to ascertain the abnormalities in the pre-set standards or provide early warning identification of hazards (Raju et al., 2017)

The proposed power efficient, simple solution *in-situ* monitoring solution is set to provide near real time analysis and dissemination of LSAT and LSWT collected. The system is also designed to connect to a remote user and provide them with an alert based on the pre-configured thresholds. E.g., Lake Water Authorities who are remotely located in the offices when there is a significant deviation of LSAT and LSWT from the pre-defined set of standard values which is an associated with a bloom.

Integration of various methodologies such as the Risk Quotient Approach to show color coded hazards and each hazard level for each parameter assessed at each location e.g., Surface temperature at a given location mapped using Geographical Information Systems (Wan M. et al, 2019).

Location-based approach in assessing lake and water resource pollution has been implemented by Waspmote in Georgia, USA (Waspmote). Sample points were established using field survey, lab analyses and geospatial techniques to monitor the various water quality parameters. The results were tables, graphs and maps showing the concentrations of the parameters.

Boddula et al. (2017) proposed a wireless sensor system, CyanoSense, which provided a low footprint, low power and low-cost solution for the monitoring algal bloom remotely in Lake Oconee, Georgia, USA.

A Smart GIS-based in-situ model for assessing aquifer vulnerability was implemented in Kakamigahara Heights, Gifu Prefecture, central Japan (Babiker et al. 2010)

A GIS-based emergency response system for sudden water pollution was developed in China. (Ma, Xu, and Wang 2014; Zhang 2014). It uses GIS technology and a hydraulic water quality model to represent the levels and extents of pollution. Maps showing the spatial distribution of the sample points are generated.

3. Materials and methods

3.1 Study area

Lake Victoria, with an extensive surface area of about 68,800 KM^2 and an average depth of 40m at a maximum depth of 79m ranks the second largest fresh water lake in the world after Lake Superior and the Largest in Africa. Lying between 3° S to 0° 30`N latitude and 31$^o$ 40`E to 34° 50`E is distributed among these three East African countries viz Tanzania 51%, Uganda 43% and Kenya the remaining 6% (africangreatlakes.org).

That in place, the lake is privileged to serve as economical home of about 40 million residents (Calamari et al.,1995) in those riparian reserves. These millions of individuals solely bank on the lake for all aspects of their daily economic livelihood ranging from, fishing, agriculture, and industrial applications just to barely highlight but a few. On that regard, it's ecological monitoring should be of great geoscientific interest.

Being located in Equatorial regions of the globe, the lake has an alternating climatic condition varying from tropical rain forest with rainfall over the lake for a better portion of the year to a semi dry climate with sporadically discontinuous droughts over some locations.

This provides ambient temperatures varying between 12-26°C which therefore provides an optimum host condition for the growth and development of the *Cyanobacteria spp.* in this scope (Okello et al., 2011).

Figure 5 shows the location and extent of the extract of the study area particularly relevant to this study.

LAKE VICTORIA

Fig. 5 Map of Winam Gulf with study sites.

3.2 Data

Five (5) datasets are exploited in this study as displayed in table 1 below.

1. From Landsat 8 Operational Land Imager Sensor from where spectral bands 2 to 5 centered on Blue $_{(480\ nm)}$, Green$_{(560nm)}$, Red $_{(655\ nm)}$ and NIR $_{(865\ nm)}$ will be used in the extraction of Chl-a.
2. Thermal data extracted from the L8 TIR sensor from which TIR1$_{(10,895nm)}$ band10 will be for the extraction of LSAT.
3. In-situ field data form the KMFRI department to aid validate the remote sensing processes.
4. ESRI GIS Shapefiles for delineation of study areas
5. In-situ data from the locally deployable autonomous IoT sensors.

Table 1: Data Sources and their roles

Data Type	Source	Role/Use
Landsat 8 OLI (30m, 16 days)	Google Earth Engine (2015-2021)	Spatiotemporal HAB Monitoring
Landsat 8 TIR (100m, 16 days)	Google Earth Engine (2015-2021)	Lake Surface Water Temperature Monitoring (LSWT)
Meteorological Data	Kenya Marine & Fisheries Research Institute-KMFRI (2015-2021)	Water Quality assessment
Shapefiles	Geodatabase of Global Administrative areas- GADM	Delineate the Study area
In-Situ Data	In-situ Sensors 2021 Onwards	Continued In-Situ Algal Monitoring

Table 2: Tools and Materials used in the study

Tool/Material	Role	Availability
Google Earth Engine (GEE)	Download and Processing	Freely Available
QGIS, R	Further Analysis & Maps	Free
Microcontroller & Sensors	In-Situ data Monitoring	Local Purchase

3.3 Methodology

3.3.1 Chl-a Estimation from Landsat 8 OLI

3.3.1.1 Relevance of Landsat-8 in Cl-a estimation

The L8 satellite supplies multispectral images comprising of 11 spectral bands, 9 in the Optical imaging region and 2 in the Thermal region (USGS). Chl-a is known to have distinctly prominent absorption behavioral patterns between certain wavelengths of the visible portion of the EM spectrum within which this space vehicle image. Notably, around the blue (450 - 475 nm) and red (650-675nm) regions, Chl-a exhibits high absorption tendency. Further, at the green and NIR regions of the EM spectrum, Chl-a exhibits high reflectance values that could reach 500 and 700 nm, respectively (Beck et al., 2016; Tuuli et al., 2020). This information has been widely exploited by researchers to develop Chl-a quantification algorithm, (Richard et al., 2018) and this study is not an exception. The presence of narrower bandwidths and at a finer spatial resolution of 30m improves L8's pigment discrimination ability even in water bodies despite the fact that it was purposely designed for terrestrial applications (Pahlevan et al., 2014). Further, the second Thermal InfraRed (TIR) sensor on board L8 provides for the measuring of the Lake Surface Air Temperature which is another significant proxy for HABs that is investigated in this study.

3.3.1.2 Satellite Data Preprocessing

Landsat-8 OLI level-1 collection-1 data product consists of quantized and calibrated scaled DN values. Retrieval of Chl-a from Landsat-8 sensor over the study region involved the following three steps,

(i) Obtaining absolute scaled DN values for all the required bands (B2, B3, B4 and B5).

(ii) The images were then subjected for atmospheric correction to minimize the atmospheric attenuation effects in the quite humid Lake Victoria regions.

(iii) Then finally Chl-a were retrieved by utilizing Ocean Chlorophyll (OC) algorithms (OC-2 shown in equation 1 below).
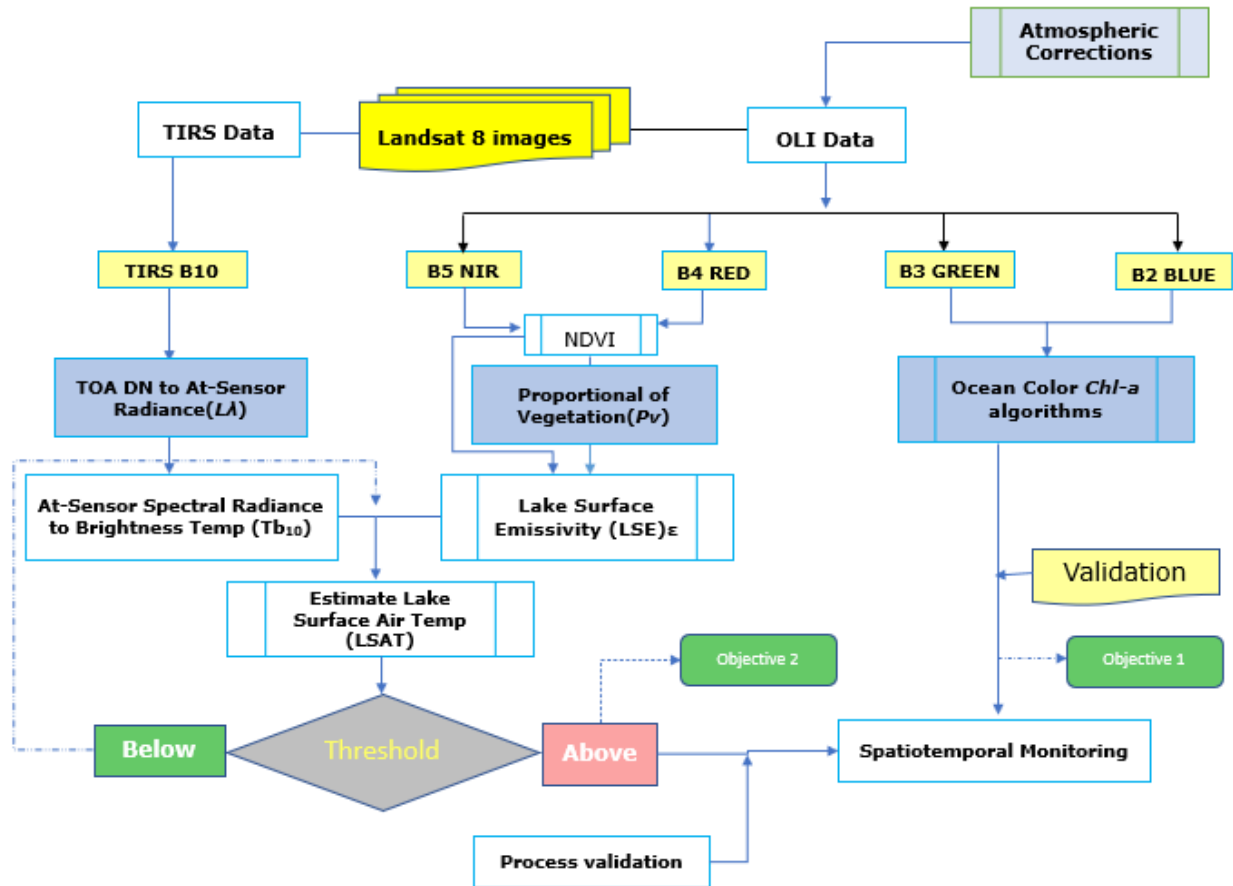
Fig 6: Overall Methodology Workflow for Objectives 1 and 2

3.3.1.3 Estimating Chl-a Concentration

Based on band positioning in the OLI sensor and previous good performance in retrieval of chl-a in inland waters (Augusto-Silva et al.,) Ocean Color 2 (OC2) algorithm was settled upon for this retrieval purpose.

OC-2 is a modified fourth order polynomial algorithm which was originally developed for the SeaWiFS data (O'Reilly et al., 1998) but can be tuned to perform relatively well with Landsat 8 (Watanabe et al., 2017; Richard et al., 2018)

Mathematically, OC-2 is an empirical two-band ratio algorithm (NASA 2011) for the quantitative estimation of chl-a and is given by:

$$\mathrm{Chl-a} = 10^{(0.2511-2.0853R+1.5035R^2-3.1747R^3+0.3383R^4)}$$ .... (eq. 1)

Where $\mathrm{R} = \log_{10} \mathrm{Rrs}(490)\big/\mathrm{Rrs}(555)$ .... (eq. 2)

Where:

Ch-a is the quantified value of Chlorophyll-a

R is the quantifying coefficient derived from the spectral bands

Rrs is Reflectance in the specified wavelength region

For OC-2, ratio of Rrs at Blue band at wavelength 490nm and Rrs Green band at 555nm are used to estimate the chl-a as reported in the following dates.

Year	Date and Month	Reporting body
2015	12th January, 22nd February	Nasa Earth data, KMFRI
2016	23rd July	KMFRI
2017	04th August	Africa great Lakes
2018	27th January	KMFRI, Nasa Earth Data
2019	18th August	KMFRI
2020	29th August,	KMFRI
2021	No Data	None Reported

Table 3: HABs reported in Lake Victoria, (KMFRI, RCMRD NASA Earth Data)

The results from the chl-a estimations from this algorithm as presented section 4 of this write-up.

3.3.1.4 Accuracy Assessment

To validate the obtained chl-a values, chl-a validation data will be retrieved from KMFRI and some from NASA Giovanni Chlorophyll-a portal, managed by Nasa Earth Data. This portal has been for so long a rich archive for global chl-a generated from MODIS, Sentinel-3 OCLI, SeaWiFS just to mention but a few. Chl-a for the study area for years 2015 through 2021 will be acquired. The spatially enabled data will then be used to assess the accuracy of the estimated Chl-a from Landsat 8 OLI.

The statistical metrics used for validation will be coefficient of determination (R^2) and Root Mean Square Error (RMSE) given by the equations 3 and 4 below respectively

$$R^2 = \frac{\sum\left(Modeled_{Chl-a,i} - Mean_{Chl-a,i}\right)^2}{\sum\left(Actual_{ActChl-a,i} - Mean_{ActChl-a,i}\right)^2} \quad \text{..............................} \text{ (eq. 3)}$$

$$RMSE = \sqrt{\frac{\sum_{i=1}^{n}\left(X_{Validation,i} - X_{L8,i}\right)^2}{n}} \quad \text{................................} \text{ (eq. 4)}$$

where $Modeled_{Chl-a,i}$ is the estimated Chl-a at point *i*, $Mean_{chl-a,i}$ is the mean of the modeled chl-a from Landsat 8 at point *i*, $Actual_{ActChl-a,i}$ represents the reference chl-a at points *i*, while $Mean_{ActLChl-a}$ is the average of the sampled actual chl-a.

$X_{Validation,i}$, is the referenced chlorophyll-a concentration at point *i*, $X_{L8,i}$ is the modeled estimate of Chl-a concentration from Landsat 8 at point *i*, n represents the total number of sampled points for validation.

3.3.2   Lake Surface Air Temperature Estimation from Landsat 8 OLI

This part of the methodology workflow mainly intends to estimate the LSAT as another proxy of HABs (Owen M et al., 2017)

3.3.2.1 Relevance of Landsat-8 in retrieval of LSAT

Thomas et al. (2012), after extensive research in the aquatic environments, observed that certain thermal conditions favor the growth, stability and spread of a wide variety of algal species. Further, after their domination and colonization, these microscopic and photosynthetically active organisms increase the LSAT of the region.

L8 TIR supplies two thermal bands (10 and 11) for the retrieval of LSAT. Wang et al. (2015) proposed the Mono-Window Algorithm for the retrieval of Land surface Temperature using the Landsat 8 band 10. Moreover, this algorithm scores equally acceptable when applied in the retrieval of LSAT in inland water bodies, hence the adoption of the same in this study. It should however be noted that data from the Landsat 8 TIRS Band 11 have large uncertainty and Wang et al., (2015) suggested the use of TIRS band 10 data as a single spectral band for LSAT estimation; for this reason, present work provides the use of L8 band 10 alone.

The information acquired is processed in a multi-software platform, in order to calculate the lake surface temperature. For this purpose, R programming environment and ArcGIS 10.8 were used.

For the successful retrieval of LSAT, the study includes the major following steps as indicated in the workflow presented in (Figure 7). That is: -

- Conversion of L8 DN pixel values to at-sensor spectral radiance ($L\lambda$)
- Transformation of at-sensor spectral radiance to at-sensor brightness temperature (Tb_{10})
- Estimation of Lake Surface Emissivity
- Estimation of Lake Surface Air Temperature by adopting MW algorithm (Wang et at., 2015).

3.3.2.2 Retrieval of Lake Surface Air Temperature

3.3.2.2.1 TOA spectral radiance ($L\lambda$)

The first step is to convert the raw DN (Digital Number) values of band10 to obtain the TOA (top of atmospheric) spectral radiance ($L\lambda$) by multiplying the multiplicative

radiometric rescaling factor (**ML**) of TIR bands with its corresponding TIR band and adding additive rescaling factor (**A_L**) using equation (5) below

$$L\lambda = ML * QCal + A_L \text{----------------------- (5)}$$

Where:

Lλ is the spectral radiance in $^{watts}/_{(m-2\,srad-1\,\mu m-1)}$

ML is the $Band_{10}$ multiplicative rescaling factor obtained from metadata (e.g.,0.0003342);

QCal is the DN value for the quantized and calibrated standard product pixel of band 10.

A_L is the band-specific additive rescaling factor obtained from the metadata (0.1);

3.3.2.2.2 Brightness temperature (Tb$_{10}$) in °C

As Latif 2014 puts it, brightness temperature is the Electromagnetic Radiance travelling upward from the top of the Earth's atmosphere. Therefore, The Brightness Temperature is not a temperature on the ground rather is the temperature at the satellite (M Z Dahiru et al., 2020). The spectral radiance value **Lλ** obtained in equation (5) above, was then converted to brightness temperature BT by adopting equation (6) below

$$Tb_{10} = \frac{K2}{Ln\left[\left(\frac{K1}{L\lambda}\right)+1\right]} - 273.15 \text{----------------------- (6)}$$

Where:

Tb$_{10}$ is the brightness temperature;

K1 and K2 are thermal constants, obtained from the metadata file of the L* OLI;

Lλ is top of atmospheric radiance.

3.3.2.2.2. Normalized Difference Vegetation Index-NDVI

This mathematical algorithm which ranges between -1.0 to +1.0 is essential to identify different land surface cover types of the study which is further necessary to calculate proportional vegetation (Pv) and Lake Surface Emissivity (ε) (M Z Dahiru et al., 2020). NDVI is calculated on per-pixel basis as the normalized difference between the red band (0.64 - 0.67μm) and near infrared band (0.85-0.88μm) of the images using the formula in equation (7) below.

$$\text{NDVI} = \frac{\text{NIR} - \text{RED}}{\text{NIR} + \text{RED}} \text{ ----------------------- (7)}$$

3.3.2.2.3 Proportion of Vegetation (Pv)

The NDVI for the study area derived from equation (7) above is then used to estimate the thermal emitting target under each land cover type denoted as proportional vegetation which is a direct function of NDVI.

The vegetation and bare soil proportions are acquired from the NDVI of pure pixels.

Pv was calculated using the equation (8) below.

$$\text{Pv} = \left[\frac{\text{NDVI} - \text{NDVImin}}{\text{NDVImax} - \text{NDVImin}} \right]^2 \text{ --------------------- (8)}$$

3.3.2.2.4. Lake surface emissivity (ε)

This is the radiative properties of objects which characterizes the ability of a body to emit thermal radiation energy across the surface into the air atmosphere (Rhinane et al. 2012). The knowledge of lake surface emissivity is further exploited to estimate surface temperature as shown in equation (9) below

$$\text{E} = 0.004 * \text{Pv} + 0.986 \text{ ---------------- (9)}$$

3.3.2.2.5. Lake Surface Air Temperature (LSAT)

We finally calculate the retrieval of LSAT using brightness temperature (BT) obtained from band 10 and Lake Surface Emissivity derived above.

LSAT has a linear relationship with at sensor brightness temperature and Lake Surface Emissivity and can therefore be retrieved using the equation (10) below:

$$\text{LST} = \frac{\mathbf{Tb}10}{\{1 + [(\boldsymbol{\lambda}\mathbf{Tb10})]|_\rho * \text{Ln}(\varepsilon)\}} \text{ -------------- (10)}$$

Were,

LST is the LST in Celsius (˚C),

$\mathbf{Tb}10$ is at- sensor BT (˚C),

λ is the average wavelength of band 10,

ε is the emissivity calculated from equation (v) above

This methodological workflow algorithm finally derives Lake Surface Air Temperature for the region under study and the results are to be presented in section 4 of this write-up.

3.3.2.2.6 Accuracy Assessment

To validate the obtained LSAT values, validation data will be retrieved from Sentinel 3 OLCI which collects global Sea Surface Temperature as one of its products. Lake Surface Air Temperature for the study area for years 2015 through 2021 will be acquired to assess the accuracy of the derived LSAT.

The statistical metrics used for validation will be coefficient of determination (R^2) and Root Mean Square Error (RMSE) given by the equations below respectively

$$R^2 = \frac{\sum\left(Modeled_{LSAT,i} - Mean_{LSAT,i}\right)^2}{\sum\left(Actual_{LSAT,i} - Mean_{ActLSAT,i}\right)^2} \quad .... \text{(eq. 11)}$$

$$RMSE = \sqrt{\frac{\sum_{i=1}^{n}\left(X_{Validation,i} - X_{L8,i}\right)^2}{n}} \quad .... \text{(eq. 12)}$$

where $Modeled_{LSAT,i}$ is the estimated LSAT at point *i*, $Mean_{LSAT,i}$ is the mean of the modeled LSAT from Landsat 8 at point *i*, $Actual_{LSAT,i}$ represents the reference LSAT at points *I*, while $Mean_{ActLSAT,i}$ is the average of the sampled actual LSAT.

$X_{Validation,i}$, is the referenced LSAT at point *i*, $X_{L8,i}$ is the modeled estimate of LSAT from Landsat 8 at point *i*, n represents the total number of sampled points for validation.

3.3.3 Automated In-situ Internet of Things System

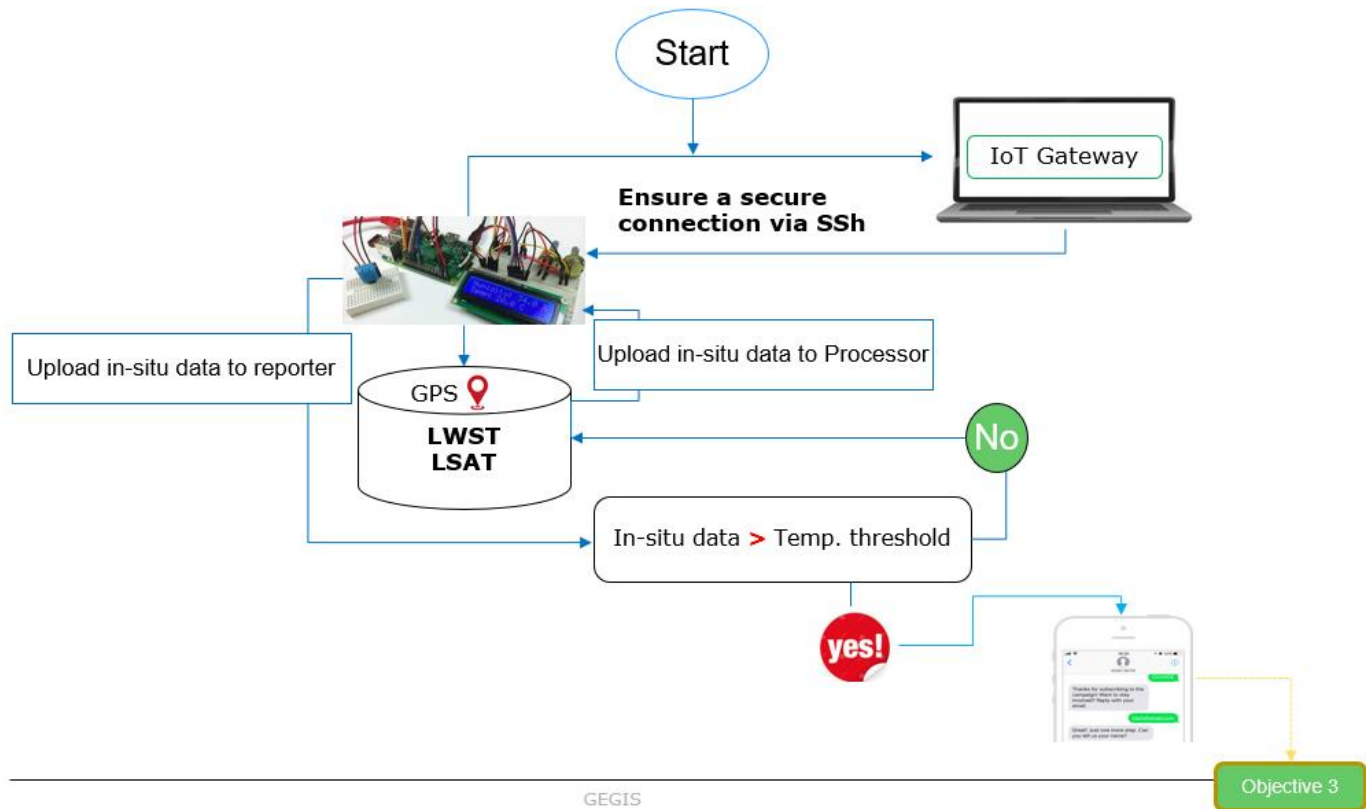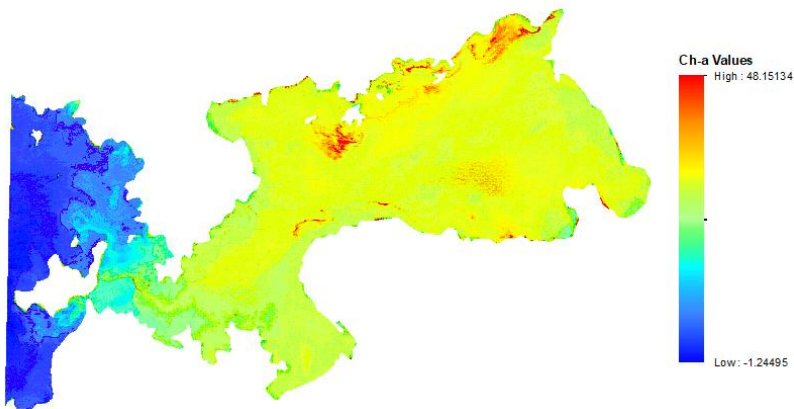The detailed methodological workflow under this section is still under review and evaluation.

Fig 7: Overall Methodology Workflow for Objectives 3
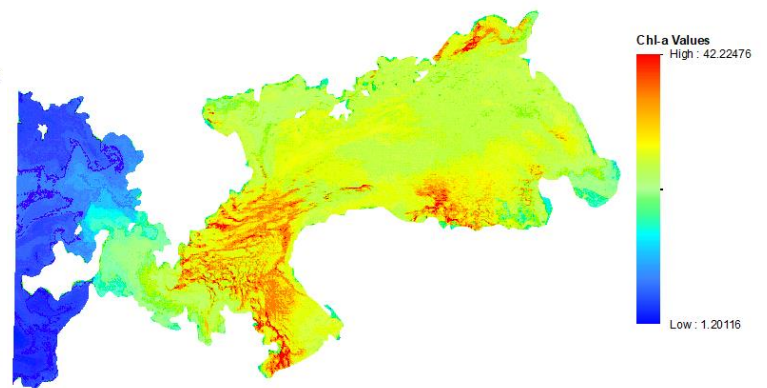
4. RESULTS

4.1 Chl-a Distribution Maps

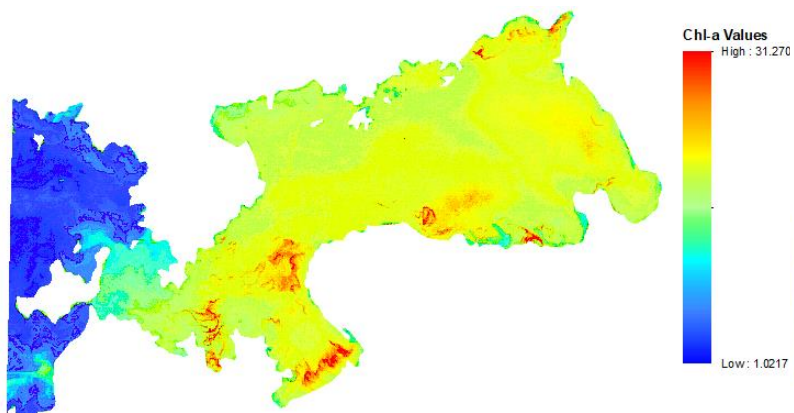Based on the above methodological progress, the following results were obtained
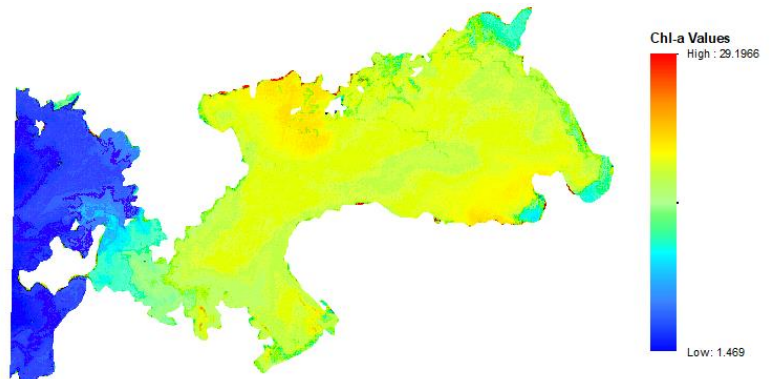
12th January 2015

22nd February 2020

23rd June 2016

04th August 2017

References

Allan, M. G., Hamilton, D. P., Hicks, B., and Brabyn, L. (2015). *Empirical and semi-analytical chlorophyll-a algorithm for multi-temporal monitoring of New Zealand lakes using Landsat*. Environ. Monit. Assess. 187, 364. https://doi.org/10.1007/s10661-015-4585-4

Anderson, D.M., Glibert, P.M., Burkholder, J.M., (2002). H*armful algal blooms and eutrophication: nutrient sources, composition, and consequences*. Estuaries 25, 704–726. Babin, M., Roesler, C.S., Cullen, J.J., 2008. Real-time Coastal Observing Systems for Marine Ecosystem Dynamics and Harmful Algal Blooms: Theory, Instrumentation and Modelling. UNESCO.

Anderson, J.; Wilson, S. (1984) *The physical basis of current infrared remote-sensing techniques and the interpretation of data from aerial surveys*. Int. J. Remote Sens., 5, 1–18.

Augusto-Silva, P.B.; Ogashawara, I.; Barbosa, C.C.F.; de Carvalho, L.A.S.; Jorge, D.S.F.; Fornari, C.I.; Stech, J.L. (2014) *Analysis of MERIS reflectance algorithms for estimating chlorophyll-a concentration in a Brazilian Reservoir. Remote Sens., 6, 11689–117077.*

Babiker, Insaf, Mohamed, Mohamed, Hiyama, Tetsuya, Kato, Kikuo, (2010) *A GIS-based model for assessing aquifer vulnerability in Kakamigahara Heights, Gifu Prefecture, central Japan*.

Beck, R.A.; Zhan, S.; Liu, H.; Tong, S.T.Y.; Yang, B.; Xu, M.; Ye, Z.; Huang, Y.; Shu, S.; Wu, Q.; et al. (2016) *Comparison of satellite reflectance algorithms for estimating chlorophyll-a in a temperate reservoir using coincident hyperspectral aircraft imagery and dense coincident surface observations.* Remote Sens. Environ. 178, 15–30.

Blondeau-Patissier, D., Gower, J. F. R., Dekker, A. G., Phinn, S. R., & Brando, V. E. (2014). *A review of ocean color remote sensing methods and statistical techniques for the detection, mapping and analysis of phytoplankton blooms in coastal and open oceans*. *Progress in Oceanography*, *123*, 123–144. https://doi.org/10.1016/j.pocean.2013.12.008

Boddula, V., Ramaswamy, L., & Mishra, D. (2017). CyanoSense: *A Wireless Remote Sensor System Using Raspberry-Pi and Arduino with Application to Algal Bloom. 2017 IEEE International Conference on AI & Mobile Services (AIMS)*, 85–88. https://doi.org/10.1109/AIMS.2017.19

Budyko, M. I. (1974) Climate and Life. International Geophysics Series, vol.18, Academic Press, New York. Bugenyi, F. W. B. & Magumba, K. M. (1996) *The present physicochemical ecology of Lake Victoria, Uganda*. In: The Limnology, Climatology and Paleocl

Bukata, R. P., Jerome, J. H., Kondratyev, K. Y., and Pozdnyakox, D. V. (1995). *Optical properties and remote sensing of inland and coastal waters*. New York, NY: CRC Press

Caballero, I., Fernández, R., Escalante, O. M., Mamán, L., & Navarro, G. (2020). *New capabilities of Sentinel-2A/B satellites combined with in situ data for monitoring small harmful algal blooms in complex coastal waters*. *Scientific Reports*, *10*(1), 8743. https://doi.org/10.1038/s41598-020-65600-1

Calamari, D.; Akech, M.O.; Ochumba, P.B.O. (1995) *Pollution of Winam Gulf, Lake Victoria, Kenya: A case study for preliminary risk assessment*. Lakes Reserv. Res. Manag. 1, 89–106.

Cao, H., & Han, L. (2021). *Hourly remote sensing monitoring of harmful algal blooms (HABs) in Taihu Lake based on GOCI images*. *Environmental Science and Pollution Research*, *28*(27), 35958–35970. https://doi.org/10.1007/s11356-021-13318-6

Cao, Z., Ma, R., Duan, H., Pahlevan, N., Melack, J., Shen, M., et al. (2020). *A machine learning approach to estimate chlorophyll-a from Landsat-8 measurements in inland lakes. Rem*. Sens. Environ. 248, 111974. https://doi.org/10. 1016/j.rse.2020.111974

Chorus and J. Bartram (1999), Toxic cyanobacteria in water. A guide to their public health consequences, monitoring and management. London: E & FN Spon,388p.

Clarke, G. L., Ewing, G. C., and Lorenzen, C. J. (1970). *Spectra of backscattered light from the sea obtained from aircraft as a measure of chlorophyll concentration*. Science 167, 1119–1121. https://doi.org/10.1126/science.167.3921.1119

Cloete, N.A.; Malekian, R.; Nair, L. *Design of Smart Sensors for Real-Time Water Quality Monitoring.* IEEE Access 2016, 4, 3975–3990.

Concha, J. A., and Schott, J. R. (2016). *Retrieval of color producing agents in case 2 waters using Landsat 8.* Rem. Sens. Environ. 185, 95–107. https://doi.org/10.1016/j.rse.2016. 03.018

Diaz R, Rosenberg R (2008) *Spreading dead zones and consequences for marine ecosystems*. Science 321:926–929

Encinas, C.; Ruiz, E.; Cortez, J.; Espinoza, A. (2017) *Design and implementation of a distributed IoT system for the monitoring of water quality in aquaculture*. In Proceedings of the Wireless Telecommunications Symposium, Chicago, IL, USA.

Freitas, F. H., and Dierssen, H. M. (2019). *Evaluating the seasonal and decadal performance of red band difference algorithms for chlorophyll in an optically complex estuary with winter and summer blooms*. Rem. Sens. Environ. 231, 111228. https://doi.org/10.1016/j.rse.2019.111228

Gikuma-Njuru, P.; Hecky, R.E.; Guildford, S.J.; MacIntyre, S. (2013) *Spatial variability of nutrient concentrations, fluxes, and ecosystem metabolism in Nyanza Gulf and Rusinga Channel, Lake Victoria (East Africa)*. Limnol. Oceanogr.58, 774–789.

Gitelson, A. (1992). The peak near 700 nm on radiance spectra of algae and water: relationships of its magnitude and position with chlorophyll concentration. Int. J. Rem. Sens. 13, 3367–3373. https://doi.org/10.1080/ 01431169208904125

Glibert, P.M., Anderson, D.M., Gentien, P., Granéli, E., & Sellner, K.G. (2005). *The Global, Complex Phenomena of Harmful Algal Blooms*

Glibert P, Heil C, Hollander D, Revilla M, Hoare A, Alexander J, Murasko S (2004) *Evidence for dissolved organic nitrogen and phosphorus uptake during a cyanobacterial bloom in Florida Bay*. Mar Ecol Prog Ser 280:73–83

Gordon, H. R., Clark, D. K., Brown, J. W., Brown, O. B., Evans, R. H., and Broenkow, W. W. (1983). *Phytoplankton pigment concentrations in the Middle Atlantic Bight: comparison of ship determinations and CZCS estimates*. Appl. Optic. 22, 20–36. https://doi.org/10.1364/ao.22.000020

Gordon, H. R., Clark, D. K., Mueller, J. L., and Hovis, W. A. (1980). *Phytoplankton pigments from the nimbus-7 coastal zone color scanner: comparisons with surface measurements*. Science 210, 63–66. https://doi.org/10.1126/science.210.4465.63

Gohin F. et al., (2003) *Satellite and in situ observations of a late winter phytoplankton bloom, in the Northern Bay of Biscay*. Continental Shelf Research, vol. 23, pp. 1117–1141,

Gower, J., Lin, S., and Borstad, G. (1984). *The information content of different optical spectral ranges for remote chlorophyll estimation in coastal waters*. Int. J. Rem. Sens. 5, 349–364. https://doi.org/10.1080/01431168408948813

Guo L (2007) *Doing battle with the green monster of Taihu Lake*. Science 317:1166

Haakstad, M.; Kogeler, J.; Dahle, S. (1994) *Studies of sea surface temperatures in selected northern norwegian fjords using Landsat TM data*. Polar Res., 13.

Hallegraeff, G. M (1993). *A review of harmful algal blooms and their apparent global increase.* Phycologia 32, 79-99

Hecky, R. E., Mugidde, R., Ramlal, P. S., Talbot, M. R., & Kling, G. W. (2010). *Multiple stressors cause rapid ecosystem change in Lake Victoria. Freshwater Biology*, 55, 19–42. https://doi.org/10.1111/j.1365-2427.2009.02374.x

Huisman J, Matthijs HC, Visser PM (2005) *Harmful cyanobacteria. Aquatic Ecology Series. Springer, Dordrecht*

Irons, J. R., Dwyer, J. L., and Barsi, J. A. (2012). The next Landsat satellite: the Landsat data continuity mission. Rem. Sens. Environ. 122, 11–21. https://doi.org/10.1016/j. rse.2011.08.026

Hill, P. R., Kumar, A., Temimi, M., & Bull, D. R. (2020). HABNet: *Machine Learning, Remote Sensing Based Detection and Prediction of Harmful Algal Blooms*. ArXiv:1912.02305 [Cs, Eess]. http://arxiv.org/abs/1912.02305

Jan, F., Min-Allah, N., & Düştegör, D. (2021). *IoT Based Smart Water Quality Monitoring: Recent Techniques, Trends and Challenges for Domestic Applications*. *Water*, *13*(13), 1729. https://doi.org/10.3390/w13131729

Jiang GJ, Ma RH, Loiselle S, Su W, Cai WX, Huang CG, Yang J, Yu W (2015) Remote sensing of particulate organic carbon dynamics in a eutrophic lake (Taihu Lake, China). Sci Total Environ 532:245–254

Khalili, M. H., & Hasanlou, M. (2019). HARMFUL ALGAL BLOOMS MONITORING USING SENTINEL-2 SATELLITE IMAGES. The International Archives of the Photogrammetry, Remote Sensing and Spatial Information Sciences, XLII-4/W18, 609–613. https://doi.org/10.5194/isprs-archives-XLII-4-W18-609-2019

Khorram, S., Catts, G. P., Cloern, J. E., and Knight, A. W. (1987). *Modeling of estuarne chlorophyll a from an airborne scanner*. IEEE Trans. Geosci. Rem. Sens. 25, 662–669. https://doi.org/10.1109/tgrs.1987.289735

Kurekin, A.A., Miller, P.I., Van der Woerd, H.J., (2014). *Satellite discrimination of Karenia mikimotoi and Phaeocystis harmful algal blooms in European coastal waters: merged classification of ocean colour data*. Harmful Algae 31, 163–176

Le, C., Hu, C., English, D., Cannizzaro, J., Chen, Z., Feng, L., et al. (2013). *Towards a long-term chlorophyll-a data record in a turbid estuary using MODIS observations*. Prog. Oceanogr. 109, 90–103. doi:10.1016/j.pocean.2012.10.002

Liu JG, Yang W (2012) *Water sustainability for China and beyond*. Science 337:649–650

Luo JH, Li XC, Ma RH, Li F, Duan HT, Hu WP, Qin BQ, Huang WJ (2016) *Applying remote sensing techniques to monitoring seasonal and interannual changes of aquatic vegetation in Taihu Lake*. China. Ecol Indic 60:503–513

Manuel, A., Blanco, A., Tamondong, A., Jalbuena, R., Cabrera, O., and Gege, P. (2020). *Optmization of bio-optical model parameters for turbid lake water quality estimation using Landsat 8 and wasi-2D*. Int. Arch. Photogram. Rem.

Sens. Spatial Inf. Sci. 11, 67–72. https://doi.org/10.5194/isprs-archives-xlii-3-w11-67-2020

Markham, B., Barsi, J., Kvaran, G., Ong, L., Kaita, E., Biggar, S., et al. (2014). *Landsat-8 operational land imager radiometric calibration and stability*. Rem. Sens. 6, 12275–12308. https://doi.org/10.3390/rs61212275

Markham, B. L., Barsi, J. A., Morfitt, R., Choate, M., Montanaro, M., Arvidson, T., et al. (2015). "*Landsat 8: status and on-orbit performance*," in SPIE remote sensing. Bellingham, WA: International Society for Optics and Photonics, 963908

Matthews, M.W. et al., (2012). *An algorithm for detecting trophic status (chlorophylla), cyanobacterial-dominance, surface scums and floating vegetation in Inland and coastal waters*. Remote Sensing of Environment 124, 637–652

Mittenzwey, K. H., Ullrich, S., Gitelson, A., and Kondratiev, K. (1992). *Determination of chlorophyll a of inland waters on the basis of spectral reflectance*. Limnol. Oceanogr. 37, 147–149. *https://doi.org/10.4319/lo.1992.37.1.0147*

NASA (2011). *Landsat 7 Science Data Users Handbook Landsat Project Science Office at NASA's Goddard Space Flight Center in Greenbelt.* 186. Available online at: http://landsat.gsfc.nasa.gov/wp-content/uploads/2016/08/Landsat7_Handbook.pdf (accessed July 5, 2021).

Munday, J., and Zubkoff, P. L. (1981). *Remote sensing of dinoflagellate blooms in a turbid estuary*. Photogramm. Eng. Rem. Sens. 47, 523–531.

Neil, C., Spyrakos, E., Hunter, P. D., and Tyler, A. N. (2019). *A global approach for chlorophyll-a retrieval across optically complex inland waters based on optical water types*. Rem. Sens. Environ. 229, 159–178. https://doi.org/10.1016/j.rse. 2019.04.027

Ochumba, P.B.O. (1987) *Periodic massive fish kills in the Kenyan part of Lake Victoria. Water Qual. Bull.12* ,119-122, 130.

Okello, W., & Kurmayer, R. (2011*). Seasonal development of cyanobacteria and microcystin production in Ugandan freshwater lakes: Seasonal development of cyanobacteria and microcystin production. Lakes & Reservoirs: Research & Management,* 16(2), 123–135. https://doi.org/10.1111/j.1440-1770.2011.00450.x

O'Reilly, J. E., Maritorena, S., Mitchell, B. G., Siegel, D. A., Carder, K. L., Garver, S. A., et al. (1998). *Ocean color chlorophyll algorithms for SeaWiFS*. J. Geophys. Res. 103, 24937–24953. https://doi.org/10.1029/98jc02160

Owen M. Dohertyb, Christopher J. Goblera, Theresa K. Hattenrath-Lehmanna, Andrew W. Griffitha, Yoonja Kanga, and R. Wayne Litakerc., (2017). *Ocean warming since 1982 has expanded the niche of toxic algal blooms in the North Atlantic and North Pacific oceans.* https//doi.org/10.1073/pnas.1619575114/

Pahlevan, N., Lee, Z., Wei, J., Schaff, C., Schott, J., and Berk, A. (2014). *On-orbit radiometric characterization of OLI (Landsat-8) for applications in aquatic remote sensing*. Rem. Sens. Environ. 154, 272–284. https://doi.org/10.1016/j.rse.2014.08.001

Qin BQ, Zhu GW, Gao G, Zhang YL, Li W, Paerl HW, Carmichael WW (2010) *A drinking water crisis in Lake Taihu, China*: linkage to climatic variability and lake management. Environ Manag 45:105– 112

Qin BQ, Yang GJ, Ma JR, Deng JM, Li W, Wu TF, Liu LZ, Gao G, Zhu GW, Zhang YL (2016) *Dynamics of variability and mechanism of harmful cyanobacteria bloom in Lake Taihu, China*. Chin Sci Bull 61:759–770

Raju, K.R.S.R.; Varma, G.H.K.(2017). Knowledge based real time monitoring system for aquaculture Using IoT. In Proceedings of the 7th IEEE International Advanced Computing Conference, IACC 2017, Hyderabad, India; pp. 318–321.

Richard, J.; Richard, B.; Jakub, N.; Christopher, N.; Min, X.; Song, S.; Bo, Y.; Hongxing, L.; Erich, E.; Molly, R.; et al (2018) Evaluating the portability of satellite derived chlorophyll-a algorithms for temperate inland lakes using airborne hyperspectral imagery and dense surface observations. Harmful Algae, 76, 35–46.

Richardson, K., 1997. *Harmful or exceptional phytoplankton blooms in the marine ecosystem.* Advances in Marine Biology 31, 301–385

Rhinane H, Hilali A, Bahi H, Berrada A. 2012. Contribution of Landsat data for the detection of urban heat islands areas Case of Casablanca. J Geog Inf Syst. 04:20–26.

River, S.; Sub-Basins, S.R. (2004) *Aerial Surveys Using Thermal Infrared and Color Videography; University of California*: Davis, CA, USA.

Rundquist, D. C., Han, L., Schalles, J. F., and Peake, J. S. (1996). *Remote measurement of algal chlorophyll in surface waters: the case for the first derivative of reflectance near 690 nm*. Photogramm. Eng. Rem. Sens. 62, 195– 200.

Ryu, J.-H., Han, H.-J., Cho, S., Park, Y.-J., and Ahn, Y.-H. (2012). Overview of geostationary ocean color imager (GOCI) and GOCI data processing system (GDPS). Ocean Sci. J. 47, 223–233. https://doi.org/doi:10.1007/s12601-012-0024-4

Santoleri R. et al., "Year-to-year variability of the phytoplankton bloom in the southern adriatic sea (1998-2000): sea-viewing wide field-of-view sensor observations and modeling study," Journal of Geophysical Research, vol. 108, p. 8122, 2003

Simiyu, B., Oduor, S., Rohrlack, T., Sitoki, L., & Kurmayer, R. (2018). Microcystin Content in Phytoplankton and in Small Fish from Eutrophic Nyanza Gulf, Lake Victoria, Kenya. Toxins, 10(7), 275. https://doi.org/10.3390/toxins10070275

Sitoki, L.; Kurmayer, R.; Rott, E(2012). Spatial variation of phytoplankton composition, biovolume, and resulting microcystin concentrations in the Nyanza Gulf (Lake Victoria, Kenya). Hydrobiologia, 691, 109–122.

Smith, B., Pahlevan, N., Schalles, J., Ruberg, S., Errera, R., Ma, R., Giardino, C., Bresciani, M., Barbosa, C., Moore, T., Fernandez, V., Alikas, K., & Kangro, K. (2021). A Chlorophyll-a Algorithm for Landsat-8 Based on Mixture Density Networks. *Frontiers in Remote Sensing*, *1*, 623678. https://doi.org/10.3389/frsen.2020.623678

Smith, R. C., and Baker, K. S. (1982). *Oceanic chlorophyll concentrations as determined by satellite* (Nimbus-7 coastal zone color scanner). Mar. Biol. 66, 269–279. https://doi.org/10.1007/bf00397032

Smith, R. B., Bass, B., Sawyer, D., Depew, D., & Watson, S. B. (2019). Estimating the economic costs of algal blooms in the Canadian Lake Erie Basin. Harmful Algae, 87, 101624. https://doi.org/10.1016/j.hal.2019.101624

Snyder, J., Boss, E., Weatherbee, R., Thomas, A. C., Brady, D., and Newell, C. (2017). *Oyster aquaculture site selection using Landsat 8-derived sea surface temperature, turbidity, and chlorophyll a. Front*. Marine Sci. 4, 190. doi:10. 3389/fmars.2017.00190

Song, W., Dolan, J., Cline, D., & Xiong, G. (2015). Learning-Based Algal Bloom Event Recognition for Oceanographic Decision Support System Using Remote Sensing Data. Remote Sensing, 7(10), 13564–13585. https://doi.org/10.3390/rs71013564

Tamatamah, R. A., Hecky, R. E., & Duthie, HamishC. (2005). *The atmospheric deposition of phosphorus in Lake Victoria (East Africa)*. Biogeochemistry, 73(2), 325–344. https://doi.org/10.1007/s10533-004-0196-9

Tang, D., Kawamura, H., Oh, I. S., & Baker, J. (2006). *Satellite evidence of harmful algal blooms and related oceanographic features in the Bohai Sea during autumn 1998*. Advances in Space Research, 9.

Thomas MK, Kremer CT, Klausmeier CA, Litchman E (2012) A global pattern of thermal adaptation in marine phytoplankton. Science 338:1085–108

Tuuli, S.; Kristi, U.; Dainis, J.; Agris, B.; Matiss, Z.; Tiit, K. (2020) *Validation and Comparison of Water Quality Products in Baltic Lakes Using Sentinel-2 MSI and Sentinel-3 OLCI Data*. Sensors, 20, 742.

USGS for a changing world, what is the best band to use in my research https://www.usgs.gov/faqs/what-are-best-landsat-spectral-bands-use-my-research?qt-news_science_products=0#qt-news_science_products

Vos, W., Donze, M., and Buiteveld, H. (1986). *On the reflectance spectrum of algae in water: the nature of the peak at 700 nm and its shift with varying algal concentration*. Delft, Netherlands: Delft University of Technology, Faculty of Civil Engineering

W. Song, J.M Dola, D. Cline and G. Xiong. (2015). Learning-based algal bloom event recognition for oceanographic decision support system using remote sensing data, Remote Sensing, vol. 7, no. 10, pp. 13 564–13 585.

Wang F, Qin Z, Song C, Tu L, Karnieli A, Zhao S. 2015. An improved mono-window algorithm for land surface temperature retrieval from Landsat 8 thermal infrared sensor data. Remote Sens. 7:4268–4289

Wang, M., Liu, X., Jiang, L., Son, S., Sun, J., Shi, W., et al. (2014). "Evaluation of VIIRS ocean color products," in Ocean remote sensing and monitoring from SpaceInternational society for optics and photonics, 92610E

Wan Mohtar, W. H. M., Abdul Maulud, K. N., Muhammad, N. S., Sharil, S., & Yaseen, Z. M. (2019). Spatial and temporal risk quotient-based river assessment for water resources management. Environmental Pollution, 248, 133–144. https://doi.org/10.1016/J.ENVPOL.2019.02.011

Waspmote- Wireless Sensor Networks Open Source Platform. [https://www.cooking-hacks.com/documentation/tutorials/waspmote #waspmote ps 2 8 4](https://www.cooking-hacks.com/documentation/tutorials/waspmote)

Watanabe, F. S., Alcantara, E., Rodrigues, T. W., Imai, N. N., Barbosa, C. C., and Rotta, L. H. (2015). *Estimation of chlorophyll-a concentration and the trophic state of the Barra Bonita hydroelectric reservoir using OLI/ Landsat-8 images.* Int. J. Environ. Res. Publ. Health 12, 10391–10417. https://doi.org/10.3390/ijerph120910391

Watanabe, F., Alcantara, E., Rodrigues, T., Rotta, L., Bernardo, N., and Imai, N. (2017). Remote sensing of the chlorophyll-a based on OLI/Landsat-8 and MSI/Sentinel-2A (Barra Bonita reservoir, Brazil). An. Acad. Bras. Ciênc. 90, 1987–2000. https://doi.org/10.1590/0001-3765201720170125

Wezernak, C., Tanis, F., and Bajza, C. (1976). *Trophic state analysis of inland lakes.* Rem. Sens. Environ. 5, 147–164. https://doi.org/10.1016/0034-4257(76)90045-6

Yang, C.; Wang, X. (2011) *The water quality and pollution character in Qingshuihai lake valley-typical urban drinking water sources*. In Proceedings of the 2011 International Conference on Remote Sensing, Environment and Transportation Engineering, Nanjing, China; pp. 7287–7291

Yin, X., & Nicholson, S. E. (n.d.). *The water balance of Lake Victoria*. 23.

Zhao, Y., Liu, D., & Wei, X. (2020). *Monitoring cyanobacterial harmful algal blooms at high spatiotemporal resolution by fusing Landsat and MODIS imagery*. *Environmental Advances*, *2*, 100008. https://doi.org/10.1016/j.envadv.2020.100008

Appendix

Add any extra materials that could not fit in the main text of your write up and is relevant to your study.